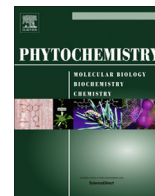




Contents lists available at ScienceDirect

Phytochemistry

journal homepage: www.elsevier.com/locate/phytochem

Ambient ionization mass spectrometry imaging of rohitukine, a chromone anti-cancer alkaloid, during seed development in *Dysoxylum binectariferum* Hook.f (Meliaceae)

P. Mohana Kumara^a, Amitava Srimany^a, G. Ravikanth^b, R. Uma Shaanker^{b,c}, T. Pradeep^{a,*}

^a DST Unit of Nanoscience (DST UNS) and Thematic Unit of Excellence (TUE), Department of Chemistry, Indian Institute of Technology Madras, Chennai 600036, India

^b Ashoka Trust for Research in Ecology and the Environment, Royal Enclave, Srirampura, Jakkur, Bengaluru 560064, India

^c Department of Crop Physiology and School of Ecology and Conservation, University of Agricultural Sciences, GKVK, Bengaluru 560065, India

ARTICLE INFO

Article history:

Received 23 September 2014

Received in revised form 4 February 2015

Available online xxxxx

Keywords:

Rohitukine

Chromone alkaloids

Dysoxylum binectariferum

Seed

DESI MS

ABSTRACT

Rohitukine, a chromone alkaloid, possesses anti-inflammatory, anti-cancer and immuno-modulatory properties. It has been reported from four species, belonging to the families, Meliaceae and Rubiaceae. Stem bark of *Dysoxylum binectariferum* (Meliaceae) accumulates the highest amount of rohitukine (3–7% by dry weight). In this study, we examine the spatial and temporal distribution of rohitukine and related compounds during various stages of seed development in *D. binectariferum* using desorption electrospray ionization mass spectrometry imaging (DESI MSI). Rohitukine (m/z 306.2) accumulation increased from early seed development to seed maturity stage. The spatial distribution of rohitukine was largely restricted to the cotyledonary tissue followed by the embryo and least in the seed coat. Besides rohitukine, rohitukine acetate (m/z 348.2) and glycosylated rohitukine (m/z 468.2) were also detected, both through mass fragmentation and exact mass analysis through Orbitrap mass spectrometry. These results indicate a dynamic pattern of chromone alkaloid accumulation through seed development in *D. binectariferum*.

© 2015 Elsevier Ltd. All rights reserved.

1. Introduction

Rohitukine (5,7-dihydroxy-8-(3-hydroxy-1-methyl-4-piperidinyl)-2-methyl-4H-chromen-4-one) (Fig. 1E), is a chromone alkaloid where the basic nitrogen ring is linked to 5,7-dihydroxy-2-methylchromone nucleus (Jain et al., 2013). The compound is reported to possess anti-inflammatory, anti-fertility, anti-implantation, anti-cancer and anti-adipogenic activities besides having immuno-modulatory properties (Harmon et al., 1979; Ismail et al., 2009; Mohana Kumara et al., 2010; Naik et al., 1988; Varshney et al., 2014). Several semi or fully-synthetic analogs of rohitukine have been developed of which flavopiridol (also known as HMR 1275 or alvocidib), is a potent CDK inhibitor with broad specificity to several kinases including CDK1, CDK2 and CDK4 (de Souza Noel, 1993). It arrests the cell cycle at both G1 and G2 phases (Senderowicz and Sausville, 2000) and has been shown to be effective against breast and lung cancers and chronic lymphocytic leukemia (Sedlacek et al., 1996; Stadler et al., 2000).

Another semi-synthetic compound, L-868276, derived from rohitukine has specific and potent inhibitory effects on CDK2 (De Azevedo et al., 1996).

Rohitukine was first isolated from leaves and stems of *Amoora rohituka* (Meliaceae) (Harmon et al., 1979). Later the alkaloid was also reported from stem bark of *Dysoxylum binectariferum* (Meliaceae) and *Schumannia phyton problematicum* and *Schumannia phyton magnificum* (both belonging to Rubiaceae) (Houghton and Hairong, 1987b; Houghton and Woldemariam, 1993; Naik et al., 1988; Yang et al., 2004). Of these sources, stem bark of *D. binectariferum* is the richest, with yields ranging between 3% and 7% by dry weight (Mohana Kumara et al., 2010). Mahajan et al. (2015) reported a substantial accumulation of rohitukine in leaves and fruits of *D. binectariferum*. Besides the plant sources, endophytic fungi associated with *D. binectariferum*, have also been reported to produce rohitukine in culture, independent of the host (Mohana Kumara et al., 2012, 2014). Recently, dysoline, a new regioisomer of rohitukine was reported from stem bark of *D. binectariferum* (Jain et al., 2013). The biosynthetic pathway of rohitukine in plants is not yet elucidated (Manske and Bossi, 1987) and the functional significance of this compound in the plant is also not clearly known.

* Corresponding author.

E-mail address: pradeep@iitmadras.ac.in (T. Pradeep).

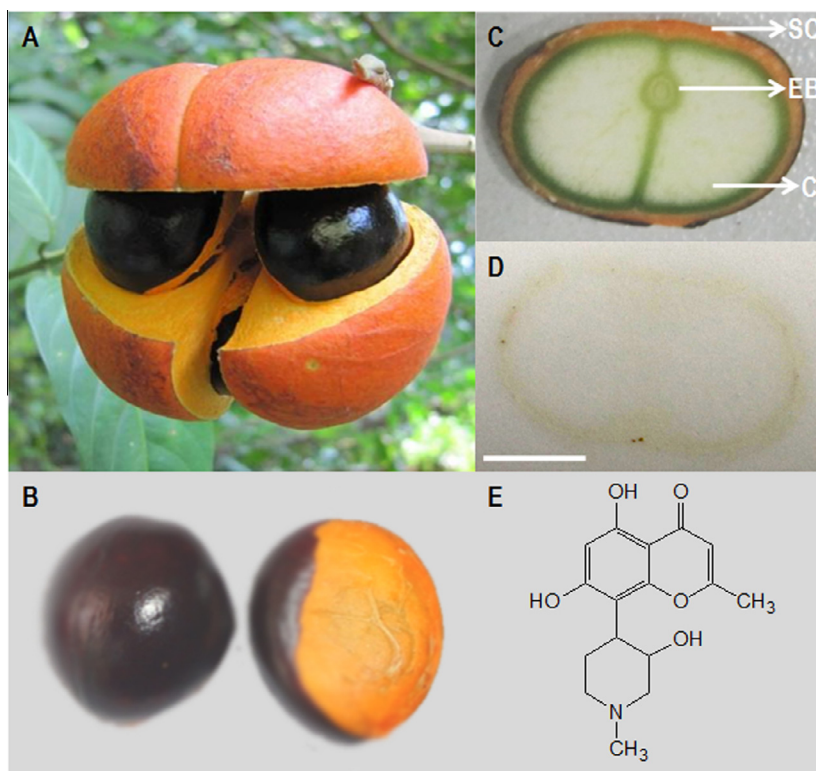


Fig. 1. (A) *Dysoxylum binectariferum* fruit showing the seeds, (B) *D. binectariferum* seed, (C) cross section of the seed through the embryonic region (SC: Seed coat, C: Cotyledon, EB: Embryo), (D) representative TLC imprint of the seed section for DESI MS imaging (scale bar is 5 mm) and (E) structure of rohitukine.

In this study, we examine the spatial and temporal distribution pattern of rohitukine and its analogs in different parts of the seeds during its development. Several studies have addressed the spatial and temporal distribution patterns of primary metabolites and nutrient loading during the seed development in agriculturally important species such as pea (*Pisum sativum*), soybean (*Glycine max*) (Bennett and Spanswick, 1983), broad bean (*Vicia faba*) (Borisjuk et al., 2002), rapeseed (*Brassica napus*) (Fang et al., 2012) and barley (*Hordeum vulgare*) (Gorzolka et al., 2014). With the advent of mass spectrometry techniques such as mass spectrometry imaging (MSI), several studies in the recent past have examined the spatial localization of secondary metabolites in various parts of plant tissue material (Bjarnholt et al., 2014; Hemalatha and Pradeep, 2013; Ifa et al., 2011; Korte et al., 2012; Kueger et al., 2012; Lee et al., 2012). For example, using desorption electrospray ionization mass spectrometry imaging (DESI MSI), efforts have been made to image several secondary metabolites (Bjarnholt et al., 2014; Hemalatha and Pradeep, 2013; Korte et al., 2012; Lee et al., 2012). In DESI MS, electrically charged solvent droplets are directed at the sample of interest to yield desorbed ions which are then conveyed into the mass spectrometer for mass analysis. DESI MS imaging technique has been used in profiling secondary metabolites in *H. vulgare* (Li et al., 2011), capsules of *Papaver somniferum* (Thunig et al., 2011), leaves of *Datura stramonium* (Thunig et al., 2011), and flower petals of *Catharanthus roseus* (Hemalatha and Pradeep, 2013), *Hypericum perforatum* (Li et al., 2013b) and seeds of *Myristica malabarica* (Ifa et al., 2011). Intriguingly, many of these studies have shown a tissue specific and heterogeneous distribution of metabolites, indicating a possible mosaic of genetic expression underlying the observed patterns. In a recent study, DESI MSI was used to show tissue specific distribution of hydroxynitrile glucosides and its relation to the expression of a key

biosynthetic enzyme in *Lotus japonicas* (Li et al., 2013a). A significant advantage of DESI is that it is an ambient ionization technique and thus, even live tissues can be analyzed.

D. binectariferum produces brightly colored fruits within which most frequently four seeds develop. On maturity, the fruits dehisce to reveal arillated seeds (Fig. 1A). Hornbills that regurgitate the seeds after eating the fat rich arils disperse the seeds (Sethi and Howe, 2012). As a typical dicot plant, each seed consists of well-defined cotyledons with an embryo and seed coat. The seeds take approximately 80–90 days to mature. For the purpose of this study, we examined the temporal patterns of accumulation of rohitukine and other related compounds during four discrete seed developmental stages and the spatial distribution of rohitukine and related compounds in different parts of the seeds through their development using HPLC, DESI MSI and ESI (Orbitrap) MS.

2. Results and discussion

2.1. Molecular ions observed from the seeds of *D. binectariferum*

DESI MS analysis of the seeds showed molecular ions signatures in the range of m/z 100–1000 for all stages of seed development (Fig. 2). Among them, the molecular ion signature of m/z 306.2 corresponding to rohitukine was predominant. DESI MS/MS analysis of the ion at m/z 306.2 yielded 3 major peaks at m/z 288, m/z 245, and m/z 222 (Fig. 3A); all of which are characteristic of rohitukine. The peak at m/z 288 is due to the neutral loss of H_2O from the piperidine ring and m/z 245 is due to further fragmentation of the ring. The peak at m/z 222 is due to fragmentation of chromone ring (Mohana Kumara et al., 2012, 2014). Besides rohitukine, a few more ions at m/z 174.1, m/z 328.2, m/z 348.2, m/z 468.2, m/z 610.5, and m/z 915.4 were identified for the first time in the seeds of *D. binectariferum* (Fig. 2). Of these, fragmentation of m/z 348.2

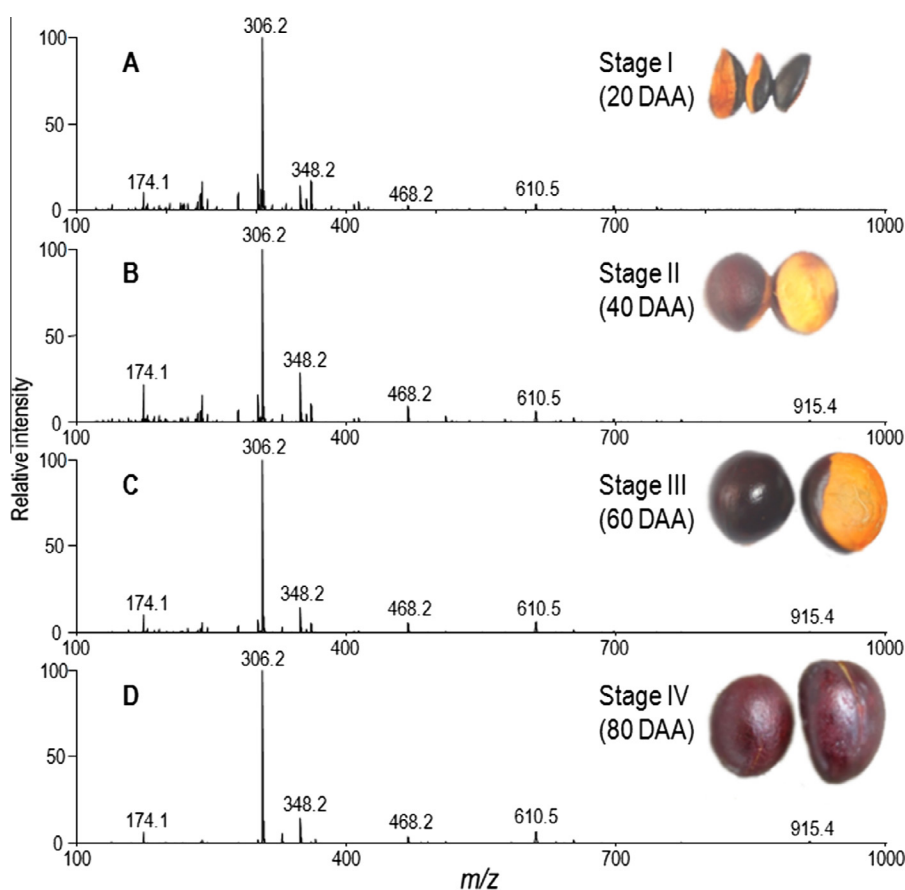


Fig. 2. DESI MS spectra of *D. binectariferum* seeds during different developmental stages. DAA refers to days after anthesis. The spectra represent the average obtained from the line scan of the images from the middle portion of the seed that contains the embryo.

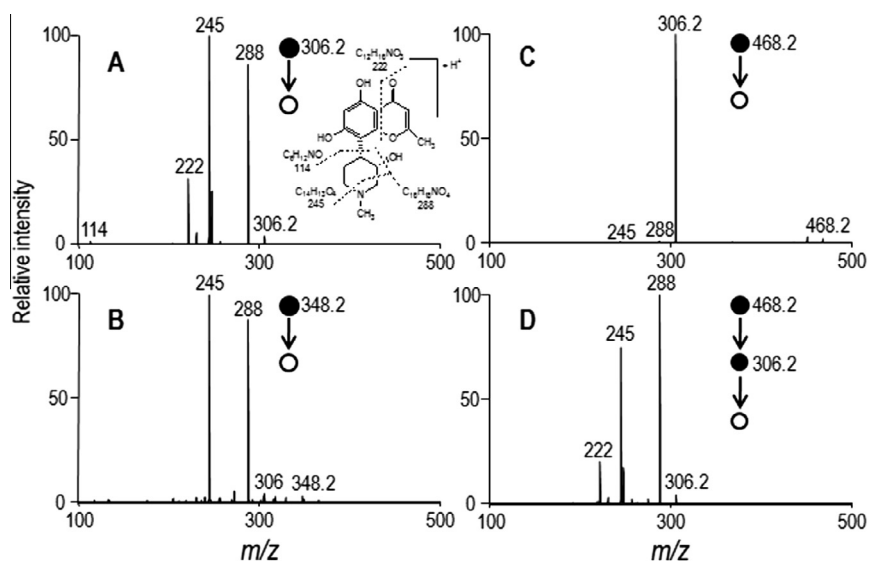


Fig. 3. Tandem DESI MS analysis of (A) rohitukine, m/z 306.2, (B) m/z 348.2, (C) m/z 468.2 and (D) m/z 306.2 (fragment ion from m/z 468.2) obtained from seeds of *D. binectariferum*. Inset in Fig. 3 (A) shows the structure of the three fragments (m/z 222, 245 and 288) obtained from rohitukine (m/z 306.2).

yielded m/z 306.2 (low relative abundance), m/z 288, and m/z 245 (higher abundances for both) (Fig. 3B), while that of m/z 468.2 yielded m/z 306.2 which upon further fragmentation yielded m/z 288, m/z 245, and m/z 222 (Fig. 3C and D). These ions are similar to those obtained on fragmenting rohitukine. Thus, it is likely that besides rohitukine (m/z 306.2), seeds of *D. binectariferum* also

contain at least two other compounds (m/z 348.2 and m/z 468.2) that could be related to the parent molecule, rohitukine. The MS/MS fragmentation of m/z 348.2 yielding m/z 306 could be accounted for by the neutral loss of ketene (CH_2CO). This ketene may have come from an acetyl group that has replaced a hydrogen atom from one of the three hydroxyl groups present in rohitukine.

Since the fragmentation pattern of m/z 348.2 is similar to that of m/z 306.2, the hydroxyl group in the piperidine ring is likely to be acetylated. For the ion at m/z 468.2, the mass difference with the ion at m/z 306.2 is 162 Da. This mass difference can be accounted by the addition of a 6-carbon sugar unit through a glycosidic bond to one of the three hydroxyl groups present in the rohitukine. Again due to a similar fragmentation pattern to that of rohitukine (Fig. 3C and D), it is likely that the sugar unit is attached with the piperidine ring.

To further confirm the identities of these ions (Fig 2), accurate m/z values of the ions were obtained by Orbitrap MS analysis. Table 1 lists the accurate m/z values of the ions with their probable chemical formulae. For m/z 348.2 and m/z 468.2, the probable chemical formulae obtained from Metlin database are due to $C_{18}H_{22}NO_6$ and $C_{22}H_{30}NO_{10}$, respectively. Based on the fragmentation patterns, these most likely correspond to acetylated and glycosylated rohitukine, respectively.

Exact mass of three other compounds (m/z 174.1237, 328.1155 and 611.2601) indicated probable chemical formulae of $C_7H_{16}N_3O_2$, $C_{16}H_{19}NO_5Na$ and $C_{32}H_{39}N_2O_{10}$, respectively, from Metlin database. While the identities of these compounds remain to be elucidated, it is likely that m/z 611.2601 corresponds to the protonated dimer of rohitukine.

2.2. Temporal and spatial patterns in the occurrence of rohitukine and related compounds during seed development – HPLC and DESI MSI analysis

On a whole seed basis, rohitukine content increased from $0.40 \pm 0.05\%$ in the second stage fruits to $0.65 \pm 0.11\%$ in the fourth stage fruits of *D. binectariferum* (Fig. 4B). Within the seed, the highest mean percentage of rohitukine was obtained in the embryo ($0.44 \pm 0.28\%$) followed by that in the cotyledon ($0.28 \pm 0.09\%$) and in the fruit coat ($0.16 \pm 0.04\%$). Fruit stalk ($0.05 \pm 0.03\%$) and seed coat (0.04 ± 0.02) yielded low levels of rohitukine (Fig. 4A).

The spatial distribution of rohitukine was largely restricted to the cotyledonary tissue followed by the embryo and lastly in the seed coat (Fig. 5). Within the cotyledonary tissue, the outer core of the cotyledon had relatively higher content of rohitukine compared to the inner core. The signatures of rohitukine were most prominent in the fourth stage seeds. The spatial and temporal distribution of m/z 348.2 (acetylated rohitukine) was similar to that of rohitukine with DESI MSI showing relatively higher abundance in cotyledon, followed by seed coat (except embryo). On the other hand, m/z 468.2 (glycosylated rohitukine) was altogether absent from the outer cotyledonary tissue as well as the seed coat. Also within the cotyledons, the distribution of m/z 468.2 was restricted to regions proximal to the embryonic axis. The ion at m/z 174.1 was uniformly distributed in the seed during the early growth stage but at seed maturity, it was patchily distributed. The spatial

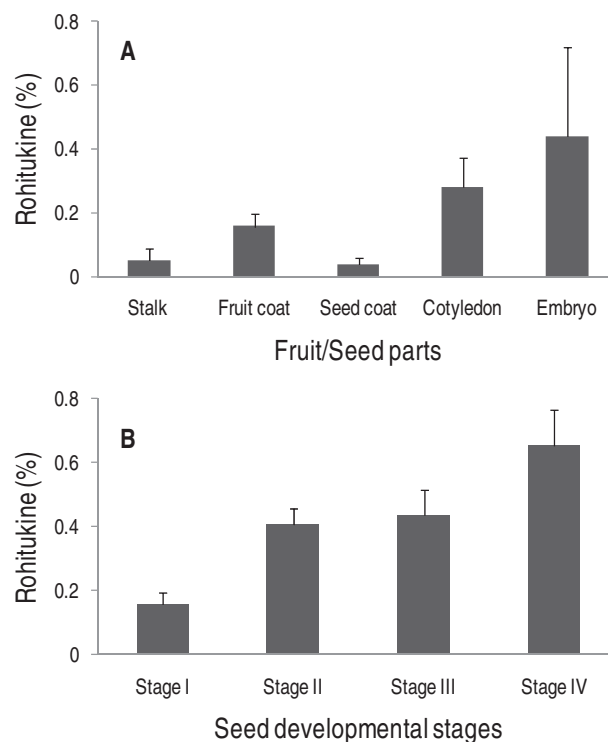


Fig. 4. HPLC analysis of rohitukine content in (A) different parts of fourth stage fruit and (B) during different developmental stages of the seeds of *D. binectariferum*. Bars indicate the standard deviation. Number of samples used for the analysis; Stalk: 4, Fruit coat: 6, Seed coat: 16, Cotyledon: 15, Embryo: 12, different stages of the seeds: 5 each.

distribution of the three ions at m/z 328.2, m/z 610.5, and m/z 915.4 was non-uniform, and tended to decrease in concentration from seed coat to the cotyledon. Distinctly, m/z 328.2 and m/z 348.2 were absent in the embryo (Fig. 5).

In order to visualize the abundance and spatial distribution of molecular ions in relation to each other, DESI MS images of pairwise molecular signatures of mature seeds (Stage IV) were superimposed. Molecular ion m/z 468.2 was localized in the central core of the seed while all other ions tended to be concentrated in the outer core of the seed. The spatial location of this ion was complementary to all other ions identified in the seed. The occurrence of m/z 174.1 was complementary to m/z 328.2, and m/z 915.4 (Fig. 6).

A number of secondary metabolites have been reported to accumulate in developing seeds, presumably to confer resistance against abiotic and biotic stress during the process of seed dispersal and germination (Alves et al., 2007; Dyer et al., 2001; McCall and Fordyce, 2010; Eriksson and Ehrlén, 1998). The secondary metabolites are either synthesized *de novo* in the seed from available precursors (Fang et al., 2012; Radchuk et al., 2011) or transported from their sites of synthesis elsewhere in the plant (Borisjuk et al., 2002; Fang et al., 2012; Patrick and Offler, 2001). In either case, there has been interest in examining the spatial and temporal pattern of accumulation of the secondary metabolites. For instance, Hebbar et al. (1993) showed that trypsin proteinase inhibitors accumulated preferentially in fruits of animal-dispersed species and not in species dispersed by wind or water. Furthermore, the accumulation of trypsin proteinase inhibitors was highest in mature but unripe fruits compared to immature and ripened fruits. They argued that the observed pattern could arise as a selection to deter predators during the mature but unripe stage, while attracting seed and fruit dispersers when the fruits were mature and ripe. In more recent studies, using DESI MSI

Table 1
Mass-to-charge (m/z) values of compounds obtained from seeds of *D. binectariferum* using DESI MS and ESI MS analysis and their probable chemical formulae.

m/z obtained from DESI MS (LTQ XL)	m/z obtained from ESI MS (Orbitrap)	Probable chemical formula of the ion	Exact m/z of the probable ion mentioned in the previous column
174.1	174.1237	$C_7H_{16}N_3O_2$	174.1237
306.2	306.1333	$C_{16}H_{20}NO_5^a$	306.1336
328.2	328.1155	$C_{16}H_{19}NO_5Na$	328.1155
348.2	348.1443	$C_{18}H_{22}NO_6$	348.1442
468.2	468.1867	$C_{22}H_{30}NO_{10}$	468.1864
610.5	611.2601	$C_{32}H_{39}N_2O_{10}$	611.2599
915.4	–	–	–

^a In this case the formula is not probable, it is exact.

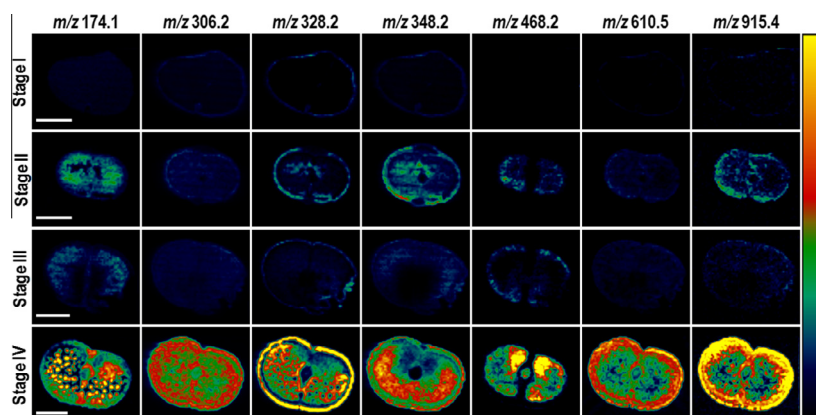


Fig. 5. DESI MS images of *D. binectariferum* seeds during different developmental stages. Intensities are normalized across the columns. The ion m/z 306.2 corresponds to rohitukine. Scale bar of 5 mm applies across each row.

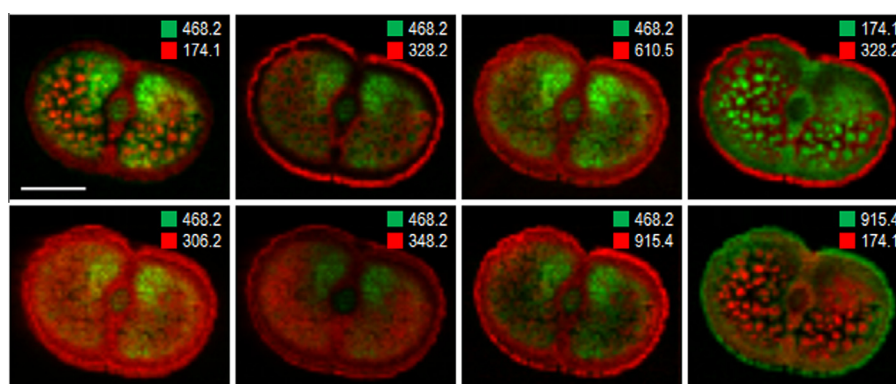


Fig. 6. Superimposed DESI MS images of the fourth stage seeds of *D. binectariferum*. Color codes refer to the specific ions given in each panel. Scale bar of 5 mm applies across each row. (For interpretation of the references to color in this figure legend, the reader is referred to the web version of this article.)

and other mass spectrometric imaging techniques, attempts have been made to spatially and temporally locate secondary metabolites in developing seeds to not only understand the compartmentalization of metabolites, if any, in different parts of the seeds, but also to trace the metabolic pathway from seed initiation to maturity (Gorzolka et al., 2014). With the advent of tissue-specific transcriptomic tools, attempts are being made to couple spatial and temporal localization with gene expression studies, to unravel critical pathway genes (Li et al., 2013a,b). In this context, our study reported here is an initial attempt to examine the spatial and temporal pattern of accumulation of rohitukine, a chromone alkaloid, in developing seeds of *D. binectariferum*. Compared to stem bark, rohitukine yield in seeds was less but substantial. Mature and ripened seeds contain about 0.6% rohitukine compared to 2–3% in stem bark. However, unlike stem bark, the seeds of *D. binectariferum* did not contain rohitukine N-oxide, an analog of rohitukine. While the biosynthetic route of rohitukine is not known, it is suggested that noreugenin (m/z 192) could be the possible upstream precursor of rohitukine (Houghton and Hairong, 1987a; Houghton and Woldemariam, 1993). However, we failed to detect noreugenin in seeds at early seed development stage, suggesting that rohitukine may be transported from sites of synthesis elsewhere in the plant to seeds. Recently, a new regioisomer of rohitukine, dysoline (m/z 306.2) was reported from stem bark of *D. binectariferum* (Jain et al., 2013). The compound differs from rohitukine in its melting point and HPLC retention time. Compared to rohitukine, the concentration of dysoline in the bark extract was very small (0.0003%) (Jain et al., 2013). In this study, we did not detect dysoline in seed tissues.

DESI MSI analysis indicated the occurrence of at least 7 distinct metabolites in seeds. Besides rohitukine (m/z 306.2), two other compounds, m/z 348.2 and m/z 468.2 representing respectively, rohitukine acetate and glycosylated rohitukine, were recovered in the seeds. These masses did not correspond to any of the reported chromone alkaloid, their analogs or natural derivatives reported from *D. binectariferum*. Four other masses of unknown identity were detected in the seeds. Two distinctive features of accumulation were observed; accumulation of rohitukine increased monotonically with seed development and there was a spatial patterning of most of the compounds in the seed. Thus rohitukine was predominantly distributed in the embryo and cotyledon with little in the seed and fruit coat. Within the cotyledon, rohitukine was fairly uniformly distributed. This is in contrast to compounds such as m/z 468.2, whose distribution was restricted to regions proximal to the embryonic axis and altogether absent from the outer cotyledonary tissue as well as the seed coat. Besides these compounds, a few others (m/z 174.1, m/z 328.2, m/z 610.5 and m/z 915.4) were also detected in the different seed developmental stages. The probable chemical formula of three of these (m/z 174.1, m/z 328.2, m/z 610.5) were obtained from the Metlin database, but their chemical structure is yet to be determined.

3. Conclusion

The present study, using DESI MSI, indicated a clear spatial and temporal distribution of rohitukine and related compounds during various stages of seed development in *D. binectariferum*. Rohitukine content increased with seed developmental stages and was largely

localized in the embryo and cotyledon, with little in the seed coat. While the evolutionary or functional significance of rohitukine in seeds is not clear, it is likely that the chromone alkaloid plays an important role as a defense compound considering the fact that rohitukine and its derivative are potent CDK inhibitors. It would be interesting to examine the underlying genetic basis of such temporal and spatial distribution of rohitukine and related compounds.

4. Experimental methods

4.1. Plant material

Fruits of *D. binectariferum* were collected from trees occurring in the Western Ghats, a mountain chain running parallel to the West coast of India and one of the 34 biodiversity hotspots of the world (Myers et al., 2000) between October 2013 and January 2014. Fruits corresponding to four developmental stages were collected, namely, immature (Stage I-20 days after anthesis), semi-mature (stage II-40 days after anthesis), matured (stage III-60 days after anthesis) and ripened (stage IV-80 days after anthesis) (Figs. 1A, B and 2). The harvested fruits were wrapped in aluminum foils and were frozen in liquid nitrogen. The frozen fruits were then transferred to a deep freezer (-80°C) for storage until further use.

4.2. Desorption electrospray ionization mass spectrometry imaging (DESI MSI)

Seeds were removed from fruits corresponding to the four developmental stages. Using a blade, the seeds were neatly cut along their minor axis (cross section) through the embryonic region, which is about 5 mm thick (Fig. 1C). The cut sections were then pressed by hand for 10 s on a hot TLC plate (TLC Silica gel 60 F₂₅₄, Merck KGaA, Germany), pre-wetted with methanol, kept on a heating mantle ($\sim 70^{\circ}\text{C}$) to get an imprint of the molecular signatures present on the cut-end of the seeds. The hand pressing method is a slight modification of an earlier method used for imprinting assisted by both solvent extraction and heating (Cabral et al., 2013). The TLC imprints were imaged using a DESI ion source. Thermo Scientific LTQ XL (Thermo Scientific, San Jose, CA, USA) mass spectrometer coupled with a 2D DESI ion source (Omni Spray Ion Source) from ProSolia, Inc., Indianapolis, IN, USA was used for imaging experiments. Methanol was used as the solvent and was sprayed at an angle of 60° to the surface. Nebulizing gas (dry nitrogen) pressure was 150 psi. Distance between the emitter and inlet was kept at 3 mm and the inlet was positioned 1 mm above the surface. Imaging area was chosen according to the sample dimensions and the spatial resolution used was $250\ \mu\text{m} \times 250\ \mu\text{m}$. Data were acquired in positive ion mode with a spray voltage of 5 kV. After acquisition of the data, they were processed by FireFly software to create the image files (IMG File) and the images were viewed using BioMap software. Collision induced dissociation (CID) was used for fragmentation of ions during MS/MS measurements.

4.3. Exact mass analysis by electrospray ionization mass spectrometry (ESI MS)

The seeds of *D. binectariferum* (Stage IV) were cut into small pieces and soaked in methanol for 12 h. Following this, the solution was filtered and centrifuged at 10,000 rpm for 10 min. The supernatant was taken for ESI MS analysis using a Thermo Scientific Orbitrap (Thermo Scientific, San Jose, CA, USA) mass spectrometer. The data were acquired in positive ion mode with a spray voltage of 5 kV.

4.4. Extraction for rohitukine and HPLC analysis

Fruits and seeds of *D. binectariferum* corresponding to the four developmental stages were oven dried for 1 week at 70°C . Rohitukine was extracted from different parts of the fruit and seeds following the protocol developed by Mohana Kumara et al. (2010). The extracted samples (20 μL) were analyzed by reverse-phase HPLC (Shimadzu, LC20AT, Japan) using RP-18 column ($4.6 \times 250\ \text{mm}$, $5\ \mu\text{m}$) with UV absorbance at 254 nm. HPLC protocol was first standardized for rohitukine using a linear gradient mode using acetonitrile and 0.1% TFA as mobile phases. We used gradient method starting from 0%:100% to 100%:0% of acetonitrile: (0.1%) TFA with a flow rate of 1 mL/min for 30 min. Sharp peak with highest peak intensity was obtained when mobile phase concentration was 30% acetonitrile and 70% TFA. All samples were then analyzed in isocratic mode using 30% acetonitrile: 70% (0.1%) TFA as mobile phase. Care was exercised to ensure that the initial and final volumes of the extract were maintained constant for the sample. Standard curve was developed for the concentration range of 0.125 mg/mL to 1 mg/mL of standard rohitukine obtained from our earlier work (Mohana Kumara et al., 2010). The best fit ($R^2 = 0.99$) was used in calculating the amount of rohitukine in the sample. All estimates were done on 5 replicates.

Acknowledgements

We thank Department of Biotechnology (DBT) and Department of Science and Technology (DST), Government of India for the financial support to carry out this work. P.M.K. thanks IIT Madras, Chennai for a postdoctoral fellowship and A.S. thanks the Council of Scientific and Industrial Research (CSIR), Government of India for PhD fellowship. We thank Prof. Graham Cooks for helpful suggestion in revising the manuscript.

References

- Alves, M., Sartoratto, A., Trigo, J.R., 2007. Scopolamine in *Brugmansia suaveolens* (Solanaceae): defense, allocation, costs, and induced response. *J. Chem. Ecol.* 33, 297–309.
- Bennett, A.B., Spanswick, R.M., 1983. Derepression of amino acid- H^+ cotransport in developing soybean embryos. *Plant Physiol.* 72, 781–786.
- Bjarnholt, N., Li, B., D'Alvise, J., Janfelt, C., 2014. Mass spectrometry imaging of plant metabolites – principles and possibilities. *Nat. Prod. Rep.* 31, 818–837.
- Borisjuk, L., Walenta, S., Rolletschek, H., Mueller-Klieser, W., Wobus, U., Weber, H., 2002. Spatial analysis of plant metabolism: sucrose imaging within *Vicia faba* cotyledons reveals specific developmental patterns. *Plant J.* 29, 521–530.
- Cabral, E., Mirabelli, M., Perez, C., Iff, D., 2013. Blotting assisted by heating and solvent extraction for DESI-MS imaging. *J. Am. Soc. Mass Spectrom.* 24, 956–965.
- De Azevedo, W.F., Mueller-Dieckmann, H.J., Schulze-Gahmen, U., Worland, P.J., Sausville, E., Kim, S.H., 1996. Structural basis for specificity and potency of a flavonoid inhibitor of human CDK2, a cell cycle kinase. *Proc. Natl. Acad. Sci.* 93, 2735–2740.
- de Souza Noel, J., 1993. Rohitukine and Forskolin. *Human Medicinal Agents from Plants*, vol. 534. American Chemical Society, pp. 331–340.
- Dyer, L., Dodson, C., Beihoffer, J., Letourneau, D., 2001. Trade-offs in antiherbivore defenses in piper cenocladum: ant mutualists versus plant secondary metabolites. *J. Chem. Ecol.* 27, 581–592.
- Eriksson, Ove, Ehrlén, Johan, 1998. Secondary metabolites in fleshy fruits: are adaptive explanations needed? *Am. Nat.* 152, 905–907.
- Fang, J., Reichelt, M., Hidalgo, W., Agnolet, S., Schneider, B., 2012. Tissue-specific distribution of secondary metabolites in rapeseed (*Brassica napus* L.). *PLoS One* 7, e48006.
- Gorzolka, K., Bednarz, H., Niehaus, K., 2014. Detection and localization of novel hordatine-like compounds and glycosylated derivatives of hordatines by imaging mass spectrometry of barley seeds. *Planta* 239, 1321–1335.
- Harmon, A.D., Weiss, U., Silverton, J.V., 1979. The structure of rohitukine, the main alkaloid of *Amoora rohituka* (Syn. *Aphanamixis polystachya*) (meliaceae). *Tetrahedron Lett.* 20, 721–724.
- Hebbar, R., Sashidhar, V.R., Shaanker, R.U., Kumar, M.U., Sudharshana, L., 1993. Dispersal mode of species influences the trypsin inhibitor levels in fruits. *Naturwissenschaften* 80, 519–521.
- Hemalatha, R.G., Pradeep, T., 2013. Understanding the molecular signatures in leaves and flowers by desorption electrospray ionization mass spectrometry (DESI MS) imaging. *J. Agric. Food Chem.* 61, 7477–7487.

- Houghton, P.J., Hairong, Y., 1987a. Further chromane alkaloids from *Schumanniohyton magnificum*. *Planta Med.* 52, 262–264.
- Houghton, P.J., Hairong, Y., 1987b. Further chromone alkaloids from *Schumanniohyton magnificum*. *Planta Med.* 53, 262–264.
- Houghton, P.J., Woldemariam, T.Z., 1993. High performance liquid chromatographic analysis of chromone alkaloids from *Schumanniohyton* species. *Phytochem. Anal.* 4, 9–13.
- Ifa, D.R., Srimany, A., Eberlin, L.S., Naik, H.R., Bhat, V., Cooks, R.G., Pradeep, T., 2011. Tissue imprint imaging by desorption electrospray ionization mass spectrometry. *Anal. Methods* 3, 1910–1912.
- Ismail, I.S., Nagakura, Y., Hirasawa, Y., Hosoya, T., Lazim, M.I.M., Lajis, N.H., Shiro, M., Morita, H., 2009. Chrotacumines A–D, chromone alkaloids from *Dysoxylum acutangulum*. *J. Nat. Prod.* 72, 1879–1883.
- Jain, S.K., Meena, S., Qazi, A.K., Hussain, A., Bhola, S.K., Kshirsagar, R., Pari, K., Khajuria, A., Hamid, A., Shaanker, R.U., Bharate, S.B., Vishwakarma, R.A., 2013. Isolation and biological evaluation of chromone alkaloid dysoline, a new regioisomer of rohitukine from *Dysoxylum binectariferum*. *Tetrahedron Lett.* 54, 7140–7143.
- Korte, A.R., Song, Z., Nikolau, B.J., Lee, Y.J., 2012. Mass spectrometric imaging as a high-spatial resolution tool for functional genomics: tissue-specific gene expression of TT7 inferred from heterogeneous distribution of metabolites in *Arabidopsis* flowers. *Anal. Methods* 4, 474–481.
- Kueger, S., Steinhauser, D., Willmitzer, L., Giavalisco, P., 2012. High-resolution plant metabolomics: from mass spectral features to metabolites and from whole-cell analysis to subcellular metabolite distributions. *Plant J.* 70, 39–50.
- Lee, Y.J., Perdian, D.C., Song, Z., Yeung, E.S., Nikolau, B.J., 2012. Use of mass spectrometry for imaging metabolites in plants. *Plant J.* 70, 81–95.
- Li, B., Bjarnholt, N., Hansen, S.H., Janfelt, C., 2011. Characterization of barley leaf tissue using direct and indirect desorption electrospray ionization imaging mass spectrometry. *J. Mass Spectrom.* 46, 1241–1246.
- Li, B., Knudsen, C., Hansen, N.K., Jørgensen, K., Kannangara, R., Bak, S., Takos, A., Rook, F., Hansen, S.H., Møller, B.L., Janfelt, C., Bjarnholt, N., 2013a. Visualizing metabolite distribution and enzymatic conversion in plant tissues by desorption electrospray ionization mass spectrometry imaging. *Plant J.* 74, 1059–1071.
- Li, B., Hansen, S.H., Janfelt, C., 2013b. Direct imaging of plant metabolites in leaves and petals by desorption electrospray ionization mass spectrometry. *Int. J. Mass Spectrom.* 348, 15–22.
- Mahajan, V., Sharma, N., Kumar, S., Bhardwaj, V., Ali, A., Khajuria, R.K., Bedi, Y.S., Vishwakarma, R.A., Gandhi, S.G., 2015. Production of rohitukine in leaves and seeds of *Dysoxylum binectariferum*: an alternate renewable resource. *Pharm. Biol.* 53 (3), 446–450.
- Manske, R.H., Brossi, 1987. *The Alkaloids Chemistry Pharmacology*, vol. 31. Academic Press Inc., San Diego, California, pp. 123–155.
- McCall, A.C., Fordyce, J.A., 2010. Can optimal defence theory be used to predict the distribution of plant chemical defences? *J. Ecol.* 98, 985–992.
- Mohana Kumara, P., Sreejayan, N., Priti, V., Ramesha, B.T., Ravikanth, G., Ganeshiah, K.N., Vasudeva, R., Mohan, J., Santhoshkumar, T.R., Mishra, P.D., Ram, V., Shaanker, 2010. *Dysoxylum binectariferum* Hook.f (Meliaceae), a rich source of rohitukine. *Fitoterapia* 81, 145–148.
- Mohana Kumara, P., Zuehlke, S., Priti, V., Ramesha, B., Shweta, S., Ravikanth, G., Vasudeva, R., Santhoshkumar, T., Spittler, M., Uma Shaanker, R., 2012. *Fusarium proliferatum*, an endophytic fungus from *Dysoxylum binectariferum* Hook.f, produces rohitukine, a chromone alkaloid possessing anti-cancer activity. *Antonie Van Leeuwenhoek* 101, 323–329.
- Mohana Kumara, P., Soujanya, K.N., Ravikanth, G., Vasudeva, R., Ganeshiah, K.N., Shaanker, R.U., 2014. Rohitukine, a chromone alkaloid and a precursor of flavopiridol, is produced by endophytic fungi isolated from *Dysoxylum binectariferum* Hook.f and *Amoora rohituka* (Roxb). *Wight & Arn. Phytomedicine* 21, 541–546.
- Myers, N., Mittermeier, R.A., Mittermeier, C.G., da Fonseca, G.A.B., Kent, J., 2000. Biodiversity hotspots for conservation priorities. *Nature* 403, 853–858.
- Naik, R.G., Kattige, S.L., Bhat, S.V., Alreja, B., de Souza, N.J., Rupp, R.H., 1988. An antiinflammatory cum immunomodulatory piperidinylbenzopyranone from *Dysoxylum binectariferum*: isolation, structure and total synthesis. *Tetrahedron* 44, 2081–2086.
- Patrick, J.W., Offler, C.E., 2001. Compartmentation of transport and transfer events in developing seeds. *J. Exp. Bot.* 52, 551–564.
- Radchuk, V., Weier, D., Radchuk, R., Weschke, W., Weber, H., 2011. Development of maternal seed tissue in barley is mediated by regulated cell expansion and cell disintegration and coordinated with endosperm growth. *J. Exp. Bot.* 62, 1217–1227.
- Sedlacek, H., Czech, J., Naik, R., Kaur, G., Worland, P., Losiewicz, M., Parker, B., Carlson, B., Smith, A., Senderowicz, A., Sausville, E., 1996. Flavopiridol (L86 8275; NSC 649890), a new kinase inhibitor for tumor therapy. *Int. J. Oncol.* 9, 1143–1163.
- Senderowicz, A.M., Sausville, E.A., 2000. Preclinical and clinical development of cyclin-dependent kinase modulators. *J. Natl Cancer Inst.* 92, 376–387.
- Sethi, P., Howe, H.F., 2012. Fruit removal by hornbills in a semi-evergreen forest of the Indian Eastern Himalaya. *J. Trop. Ecol.* 28, 531–541.
- Stadler, W.M., Vogelzang, N.J., Amato, R., Sosman, J., Taber, D., Liebowitz, D., Vokes, E.E., 2000. Flavopiridol, a novel cyclin-dependent kinase inhibitor, in metastatic renal cancer: a university of Chicago phase II consortium study. *J. Clin. Oncol.* 18, 371.
- Thunig, J., Hansen, S.H., Janfelt, C., 2011. Analysis of secondary plant metabolites by indirect desorption electrospray ionization imaging mass spectrometry. *Anal. Chem.* 83, 3256–3259.
- Varshney, S., Shankar, K., Beg, M., Balaramnavar, V.M., Mishra, S.K., Jagdale, P., Srivastava, S., Chhonker, Y.S., Lakshmi, V., Chaudhari, B.P., Bhatta, R.S., Saxena, A.K., Gaikwad, A.N., 2014. Rohitukine inhibits in vitro adipogenesis arresting mitotic clonal expansion and improves dyslipidemia in vivo. *J. Lipid Res.* 55, 1019–1032.
- Yang, D.-H., Cai, S.-Q., Zhao, Y.-Y., Liang, H., 2004. A new alkaloid from *Dysoxylum binectariferum*. *J. Asian Nat. Prod. Res.* 6, 233–236.